A 50 mm BORE SUPERCONDUCTING DIPOLE WITH A UNIQUE IRON YOKE STRUCTURE

LBL--32071

DE93 002547

* D. Dell'Orco, S. Caspi, J. O'Neill, A. Lietzke, R. Scanlan, C.E. Taylor, A. Wandesforde
Lawrence Berkeley Laboratory
1 Cyclotron Road M.S. 46-161
Berkeley, CA 94720
U.S.A.

Abstract---A 50 mm bore superconducting dipole with a thin stainless steel collar and a close in elliptical iron yoke was designed in order to obtain a high transfer function and low saturation effects on the multipoles, and a one meter model was built and tested. Training behavior of the first 1 m model, called D19, is presented at 4.3 K and 1.8 K. At 1.8 K it reached the record field of 10.06 T. The two layer cos θ winding uses 30 and 36 strand cables identical to the cables of the 50 mm bore SSC dipole and it has an operating field of 6.6 T at 4.35 K with a current of 5800 A. To evaluate behavior at high fields, the mechanical structure for the model was designed for 10 T. The thin collar itself provides only a minimum prestress of 10 MPa, and the full prestress of 70 MPa is given by the iron yoke. An aluminum spacer is used to control the gap size in the vertically split iron yoke. The tapered gap in the yoke is determined by the size of the Al spacer so that during cooldown there is no loss of coil prestress and the gap remains closed when the magnet is energized.

I. INTRODUCTION

The superconducting dipole D19 (Figures 1-2) has 20 turns in the inner layer and 29 turns in the outer layer. The cable is identical to that of the SSC Collider Dipole Magnet, having 30 strands in the inner cable and 36 strands in the outer cable; cable parameters are shown in Table 1. The cable is insulated with 0.1 mm thick kapton tape coated on one side with about 5μm of B-stage epoxy. After winding the coils with a cable tension of 300 N and curing them, 6500 N axial tension was applied to the coils using the winding mandrel. Collars were then put into place and the mandrel released so that the axial coil tension is mantained by axial compression of the collars through the collar pole pieces and the winding poles. The collars are then compressed radially in a press and interlocked by inserting the keys. The keys are tapered with a negative angle to lock them into place. The stainless steel Nitronic 40 collar consists of two symmetric pieces assembled in packs of 90 laminations, each 1.37 mm thick, which provide complete pole support (ends included) to the coils along the length of the magnet. The collar is designed to apply a prestress of 10 MPa.

The collared coils are then positioned between the two halves of the iron yoke separated by the Al bars. The iron yoke, used to maximize and to shape the magnetic field, also has structural functions; compression force is transferred to the coils via the yoke and the Lorentz forces are supported by the yoke. The yoke consists of laminations glued together in 102 mm thick blocks.

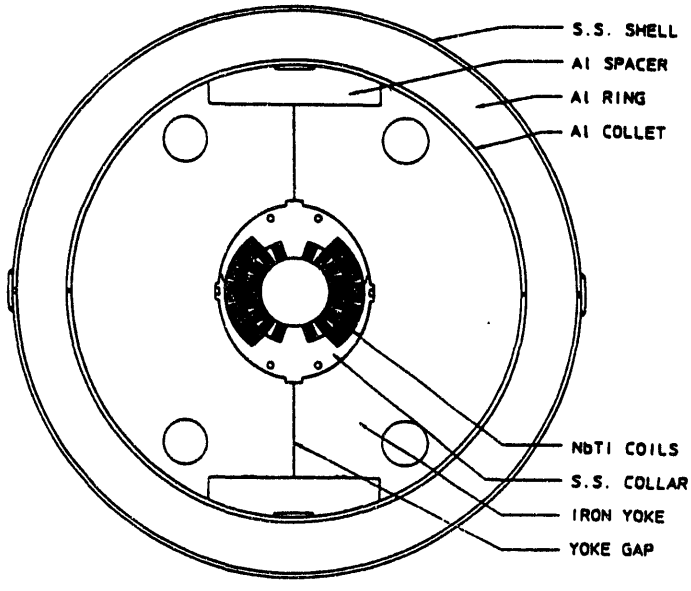

Figure 1: D19 cross section

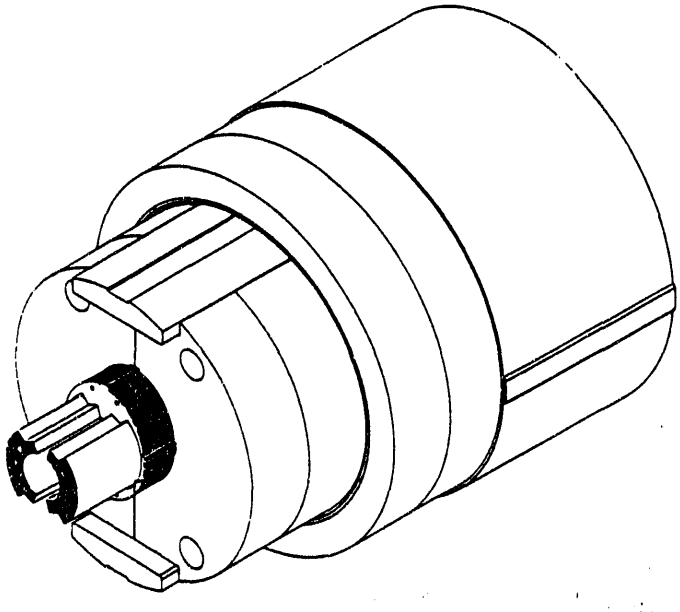

Figure 2: D19 end view

* This work was supported by the Director, Office of Energy Research, Office of High Energy and Nuclear Physics, High Energy Physics Division, U.S. Department of Energy, under Contract No. DE-AC03-76SF00098.

For the 1 m model D19, the yoke is supported by a 35 mm thick Al ring and collet structure. We selected the ring-collet suport system for its convenience and flexibility in this one-meter model. However, for accelerator applications, the external support could be provided by a shell that is squeezed against the yoke using a press and welded; A model experiment shows that structural behavior would be identical. The collets are placed over the yoke and the rings are pressed into place one at a time; since the rings and collets have a taper angle of 2° and an interference of 0.71 mm with the yoke, this drives the collets against the yoke which decreases the gap and compresses the collars and coil. As the gap is decreased the keys become unloaded, and the entire coil load is assumed by the external rings; the collars then serve as spacers. The coil prestress increases until the two halves of the yoke contact the Al bars; the yoke gap and coil prestress are determined by the size of the Al spacers. At this stage the coils have a prestress of 70 MPa. The difference in thermal contraction coefficient between the ring, yoke, and coils allows the yoke gap to close during cooldown and keeps the coil prestress constant. In this way the use of unnecessarily high coil prestress at room temperature, that could cause electrical shorts and creep in the coils, is avoided. Since the Lorentz forces at 10 T unload the yoke gap without opening it, the magnet structure is very stiff and the deformations small. 70 MPa coil prestress prevents separation between the coils and the collar when the magnet is energized to 10 T. A 4.8 mm stainless steel shell was welded around the ring over the length of the magnet to provide axial stiffness and carry the axial Lorentz load. The ends were preloaded at room temperature with a 27 kN axial compressive load.

A mechanically similar 50 mm bore two layer dipole designed to provide background field for a cable test facility (D-16B-1) was built and tested at LBL in 1988. Since high field uniformity was not required, the magnet had no collar and the iron was placed directly against the coils. The magnet first quenched at 7 T with a current of 6000 A and it reached 7.6 T at 6600 A. At 1.8 K it reached 9.2 T.

Table 1. D19 Cable Parameters

	Inner Layer	Outer Layer
No. strands	30	36
Strand diameter (mm)	0.808	0.648
Width (mm)	12.34	11.68
Thickness (mm)	1.326 1.588	1.054 1.260
Cu/Sc ratio	1.3	1.8
J_c(4.22 K, 7 T) (A/mm^2)	1716	–
J_c(4.22 K, 5.6 T) (A/mm^2)	–	2275

II. MAGNETIC ANALYSIS

The magnetic design [1] was done in two steps: an infinite permeability analysis with an analytical code assuming a circular yoke, and a real-iron analysis with the elliptical yoke using the finite element program POISSON. The ellipticity was optimized to reduce the total change in sextupole from low current to the operating current of 5800 A and field of 6.6 T. With the 165 mm yoke outer radius, similar to that of the SSC dipole, there is a decrease in sextupole at high current when the flux starts leaking out the yoke. D19 has an ellipticity of 1.14 and a change in sextupole of -0.8 units at 6.6 T due to saturation in the yoke. The close-in design allows the yoke to be near the coils at the mid plane and thus to maximize its contribution to the central field while the saturation effect on the sextupole is minimized with the ellipticity. This results in a transfer function of $1.138 \cdot 10^{-3}$ T/A, 12% higher than the 50 mm bore SSC dipole with identical cable. Although the principle of shaping the iron aperture to control the saturation effect is not new [2], to our knowledge, this is the first accelerator magnet built that way. The operating and short-sample currents at 4.35 K and 1.9 K are shown in Table 2 [3]. The calculated load lines and the short sample curves are shown in Figure 3; the central field is limited to 7.64 T at 4.35 K by the inner cable with a current of 6910 A. At 1.9 K the maximum calculated field is 9.83 T with 9400 A. At 6.6 T and 5800 A the maximum temperature is 5.17 K. The stored energy is 100 kJ/m at 6.6 T.

Table 2. D19 Design Parameters

D19	Central Field (T)	Max. Field Conductor (T)
5800 A @ 4.35 K Operating Current	6.6	6.91
6910 A @ 4.35 K Max. Current Expected	7.64	8.02
9400 A @ 1.9 K Max. Current Expected	9.83	10.38

A three-dimensional analysis with an in-house code was used to compute and mimize the multipole coefficients in the ends [4]. In order to reduce the maximum field at the cable, the iron yoke is truncated 77.5 mm short of the end of the inner layer straight section and a non-magnetic stainless steel yoke extends over the ends. The maximum field occurs at the innermost strand of the inner layer in the straight section of the pole turn.

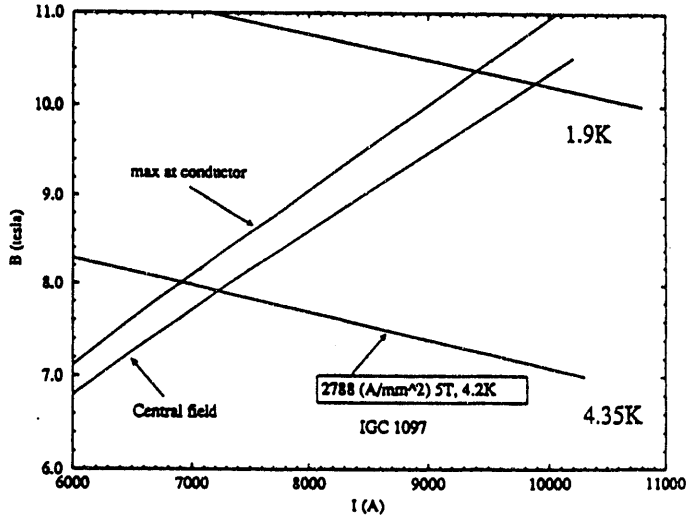

Figure 3: Load lines and short sample curves

III. MECHANICAL ANALYSIS

The finite element program ANSYS [5] was used to perform the mechanical analysis [6]. The finite element model consists of two layers: the first is magnetic and mechanical and represent one quarter of the magnet cross section; the second is only mechanical and represents the next collar lamination. The same model was used to perform both a magnetic and mechanical analysis in which the magnetic analysis is used mainly to obtain the Lorentz forces on the structure. (By using this method with a more refined mesh the magneto-mechanical analysis can be followed by a more precise field analysis to compute the effect of the deformed geometry on the multipole coefficients [7].)

The computation is iterative because as the Lorentz forces are applied to the structure and stresses and strains computed, the interface elements status (open or closed) are changed until convergency is achieved.

Three dimensional interface elements were used to model the relative sliding and separation of the different materials inside the magnet. The model contains interface elements between the coils, collar, Al bar, yoke and ring, but not between the wedges and the coils or between each turn of the coils because this is believed to be a marginal detail. The coils are joined to both the collar laminations by interfaces. The two layers of the collar are interlocked by the keys and by the pins.

The assumptions adopted in the mechanical analysis are the following: the iron has infinite permeability and no saturation; all the materials are homogeneous, and linearly elastic; the coils are orthotropic and all the other materials are isotropic; the coils have no hysteresis; there is no sliding between the coils and the copper wedges; there is no friction; plane stress analysis is valid.

The coil Youngs modulus measured with a compression test done on a stack of ten inner cables is 7800 MPa [8].

The goals of the mechanical design of this magnet are the followings: to have a yoke gap that closes during the cooldown and does not open when the Lorentz forces are applied, to minimize stresses and displacements, and to have a minimum residual compression at the poles when the magnet is energized. The yoke gap must close in order to increase the stiffness of the whole magnet, so that the Lorentz forces are applied to the yoke and not to the ring.

Five load cases were examined: collared coils; magnet at room temperature; magnet cooled to 4 K; magnet energized to 10 T (8772 A); and magnet energized to 6.6 T (5800 A).

Alignment in the yoke is obtained by means of the lower and upper collar tabs. At room temperature, after the magnet is assembled, there is a gap between the tab and the yoke equal in size to the yoke gap. This gap is necessary to allow the yoke gap to close during the cooldown. Before the yoke gap closes, initial alignment can be provided by the keyway tabs; however, as the gap closes, the keyway tabs can no longer provide positive alignment because they are moving vertically during the magnet assembly as the collars close. After cooldown, alignment in the yoke is guaranteed by the upper and lower tabs. A finite element analysis has shown that although the collar is elliptical it is not self-aligning because of its low stiffness.

Since the prestress is caused by the relative motion of the yoke with respect to the collar, it is very important to reduce the friction to assure the correct coil prestress. The friction may also oppose the alignment of the collar during cooldown. It may also cause a non-uniform stress in the ring and therefore yielding and loss of prestress during thermal cycles. In order to reduce the friction, D19 has two 0.25 mm thick stainless steel lubricated sheets between the collars and the yoke.

The ends and part of the straight section of the D19 coils are surrounded by collars without pole segments and by stainless steel laminations identical to the rest of the yoke. In order to compensate for the different thermal shrinkage the yoke gap has been reduced in these laminations by inserting a 0.12 mm thick stainless steel shim.

Table 3. D19 Lorentz Forces on a Quadrant

D19	6.6 T	10 T
F_x (N/mm)	1015	2331
F_y (N/mm)	-387	-887
F_z (N)	26800	61500

Table 4. D19 Mechanical Parameters

D19-ring & collet	magnet at 300 K	magnet at 4 K	magnet at 4 K - 6.6 T	magnet at 2 K - 10 T
$\sigma_{m.plane}$ (MPa)	-68	-70	-82	-98
$\sigma_{top\ i.c.}$ (MPa)	-72	-73	-50	-20
$\sigma_{top.\ o.c.}$ (MPa)	-69	-72	-51	-24
$F_{half\ gap}$ (N/mm)	0	2328	1951	1465
$F_{Al\ bar}$ (N/mm)	107	157	203	262
σ_{ring} (MPa)	89	172	172	172

In Table 3, the Lorentz forces acting on each block of conductors in a quadrant of D19 are shown. At 10 T, the S.S. collar at the mid plane near the keyway has a radial displacement due to the Lorentz forces of 36 mm; the radial displacement of the collar on the vertical axis is -42 mm. In Figures 4-5 the diagrams of the azimuthal stress at the pole and the mid plane of the coils are shown. The mechanical behaviour is summarized in Table 4. At the mid plane the

Lorentz force increases the prestress on the inner coil by 21 MPa and on the outer coil by 37 MPa. At the coils poles, the Lorentz forces decrease the inner coil prestress 54 MPa and the outer coil prestress by 48 MPa. It was considered important to apply enough prestress at assembly so that when the magnet is energized there is at least 20 MPa residual compression at the pole to minimize wire motion that could cause training.

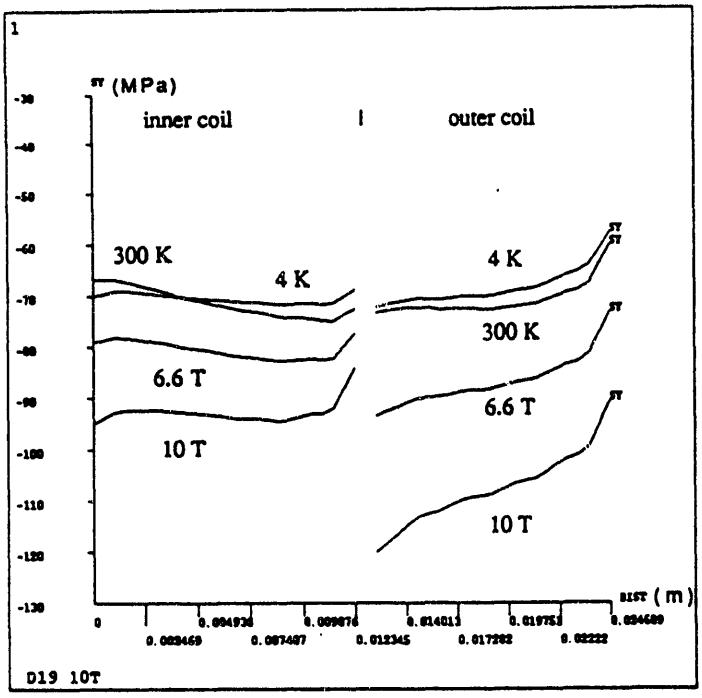

Figure 4: pressure distribution on the coils mid plane

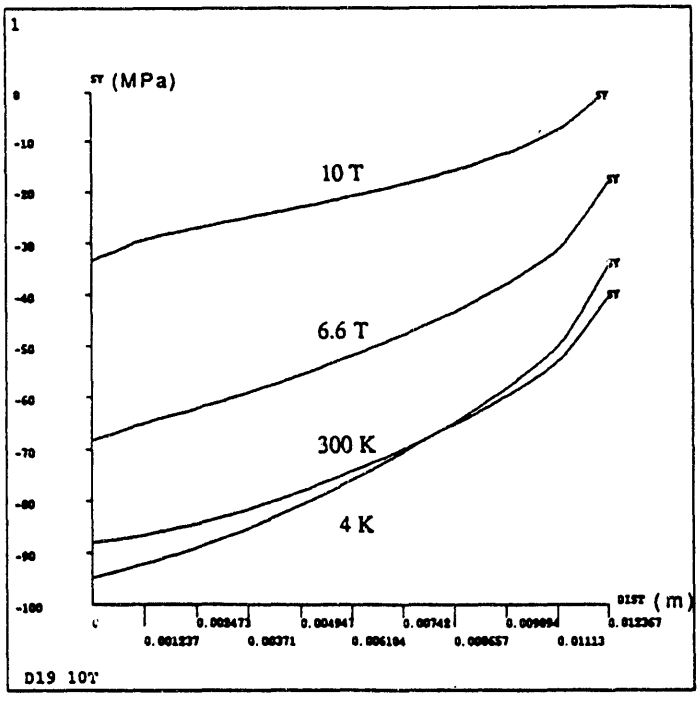

Figure 5: pressure distribution on the inner layer pole

IV. TESTING

The 1 m long magnet D19 was tested in a horizontal cryostat at 4.35 K and 1.8 K. The training history is shown in Figure 6. At 4.35 K the first quench was at 98.9 of plateau and the plateau of 7.62 T was reached on the second quench. In the second test following a warm up to room temperature, the initial quench was at 94.6% of plateau which was reached on the third quench. There was no training in a third and fourth thermal cycle. At 1.8 K the first quench was at 9.42 T, 93.6% of the 10.01 T plateau, which was reached in 9 quenches. The record field of 10.06 T was obtained after 11 quenches. These results are in agreement with the short sample prediction. The quenches were located predominantly in the inner layer pole turn near the center of the magnet. No end quenches were observed.

Sensitivity to the current ramp rate at 4.35 K between 200-1200 A/s is shown. Quench current was greater than 4500 A (Bo = 5.5 T) for ramp rates up to 1200 A/s.

Kapton insulation was slightly thicker than that used in the design calculations which explains an offset of 8 units in the low current multipoles. Figure 7 shows the variation of sextupole vs. current as built calculation and measured. Similarly the transfer function and decapole are shown in Figures 8-9. We believe the difference at current below 5 kA is probably due to presence of a weak ferromagnetism that we have observed in the elliptical collars; however, this will be verified with additional tests.

25% of the Lorentz end load was measured bearing directly on the end plates that directly support the coils ends; the remaining 75% is transfered directly to the shell through the ring and collet structure, bypassing the end plates.

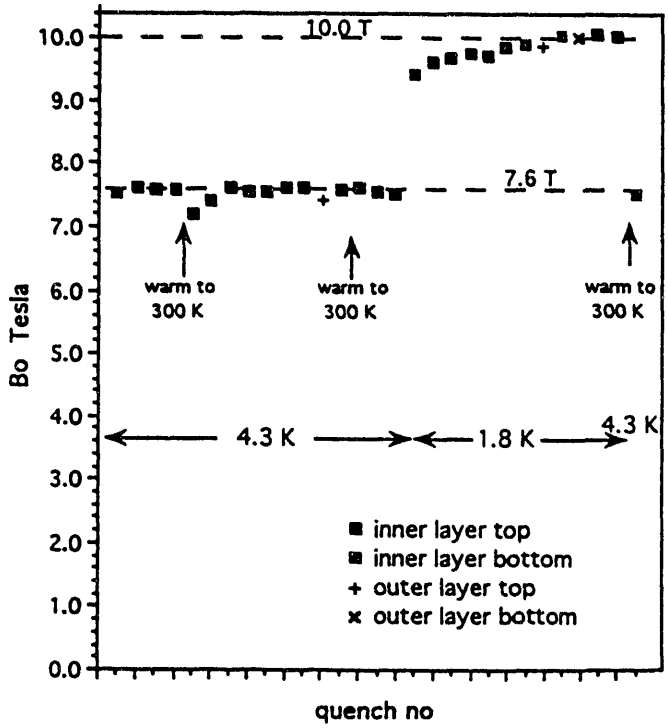

Figure 6: D19 Training at 16 A/s

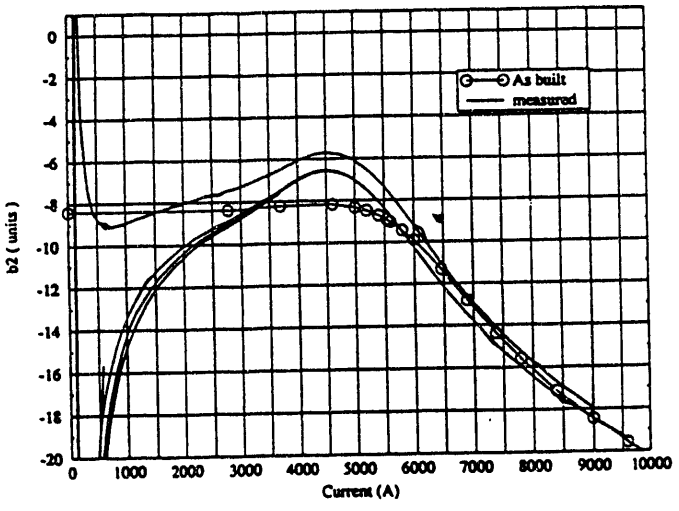

Figure 7: Sextupole variation

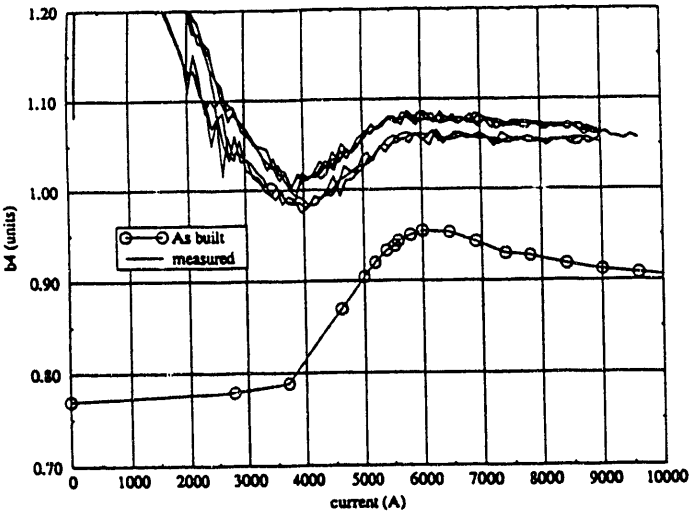

Figure 9: Decapole variation

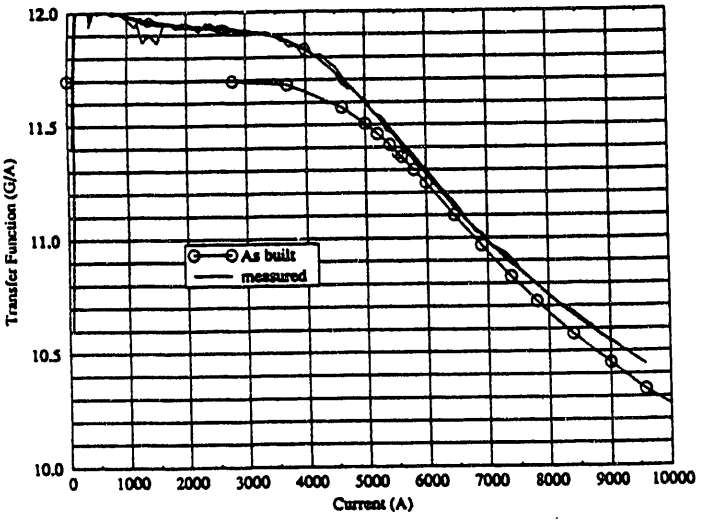

Figure 8: Transfer function

V. CONCLUSIONS

Test of dipole D19 shows the feasibility of the thin collar and the elliptical yoke concepts for accelerator magnets. Training behavior is good. Also, it demonstrates that a tapered yoke gap that closes during cooldown, controlled by an aluminum spacer, can be used to maintain constant coil prestress. The magnet is able to withstand the Lorentz forces at 10 T and will be used to test coils wound with new types of cables.

VI. ACKNOWLEDGEMENTS

The authors wish to thank S. Dardin, L. Amerman and R. Lafever for their contribution to the successfull design and construction of the magnet D19 and P.Barale and M. I. Green for the magnetic field measurements.

REFERENCES

[1] S. Caspi, A 50 mm Dipole for the SSC - DE-1, Lawrence Berkeley Laboratory, SC-MAG-283.

[2] G. Morgan, Use of an Elliptical Aperture to Control Saturation in Closely-Coupled, Cold Iron Superconducting Dipole Magnets, IEEE Trans. on Nuclear Science, Vol. NS-32, No. 5, 3695-3697, October 1985.

[3] S. Caspi, Expected Short Sample Performance of Dipole D19, Lawrence Berkeley Laboratory, SC-MAG-366.

[4] S. Caspi, M. Helm, L.J. Laslett, Magnetic Field at t h e End Region of the Dipole D19, Lawrence Berkeley Laboratory, SC-MAG-335, LBID-1735.

[5] J. A. Swanson, G. De Salvo, ANSYS Users Manual, Swanson Analysis Systems Inc. P.O. Box 65, Houston, PA 15342

[6] D. Dell'Orco, Finite Element Analysis of Elliptical Dipole Magnet D19, Lawrence Berkeley Laboratory, SC-MAG-329.

[7] D. Dell'Orco, Y. Chen, Magnetic Field Quality Analysis Using ANSYS, Lawrence Berkeley Laboratory, SC-MAG-302.

[8] E. Hiss, Mechanical Testing of D19 Cable, Lawrence Berkeley Laboratory, SC-MAG-397.

END

DATE FILMED

2/3/93